Cell Metabolism
Article

Glucose-Induced Cyclic AMP Oscillations Regulate Pulsatile Insulin Secretion

Oleg Dyachok,[1,2] Olof Idevall-Hagren,[1] Jenny Sågetorp,[1] Geng Tian,[1] Anne Wuttke,[1] Cécile Arrieumerlou,[3] Göran Akusjärvi,[4] Erik Gylfe,[1] and Anders Tengholm[1,*]
[1]Department of Medical Cell Biology, Uppsala University, Biomedical Centre, Box 571, SE-751 23 Uppsala, Sweden
[2]Department of Biophysics, Kiev T. Shevchenko National University, 01033, Kiev, Ukraine
[3]Infection Biology, Biozentrum, University of Basel, Klingelbergstrasse 50/70, CH-4056, Basel, Switzerland
[4]Department of Medical Biochemistry and Microbiology, Uppsala University, Biomedical Centre, Box 582, SE-751 23 Uppsala, Sweden
*Correspondence: anders.tengholm@mcb.uu.se
DOI 10.1016/j.cmet.2008.06.003

SUMMARY

Cyclic AMP (cAMP) and Ca^{2+} are key regulators of exocytosis in many cells, including insulin-secreting β cells. Glucose-stimulated insulin secretion from β cells is pulsatile and involves oscillations of the cytoplasmic Ca^{2+} concentration ($[Ca^{2+}]_i$), but little is known about the detailed kinetics of cAMP signaling. Using evanescent-wave fluorescence imaging we found that glucose induces pronounced oscillations of cAMP in the submembrane space of single MIN6 cells and primary mouse β cells. These oscillations were preceded and enhanced by elevations of $[Ca^{2+}]_i$. However, conditions raising cytoplasmic ATP could trigger cAMP elevations without accompanying $[Ca^{2+}]_i$ rise, indicating that adenylyl cyclase activity may be controlled also by the substrate concentration. The cAMP oscillations correlated with pulsatile insulin release. Whereas elevation of cAMP enhanced secretion, inhibition of adenylyl cyclases suppressed both cAMP oscillations and pulsatile insulin release. We conclude that cell metabolism directly controls cAMP and that glucose-induced cAMP oscillations regulate the magnitude and kinetics of insulin exocytosis.

INTRODUCTION

Glucose is the main physiological stimulus for insulin secretion from pancreatic β cells. The stimulus-secretion coupling involves metabolism of the sugar, which leads to increase of the cytoplasmic ATP/ADP ratio and closure of ATP-sensitive K^+ (K_{ATP}) channels in the plasma membrane. The resulting depolarization triggers influx of Ca^{2+} through voltage-dependent Ca^{2+} channels and exocytosis of insulin secretory granules (Henquin, 2000). The glucose-induced depolarization and Ca^{2+} influx are periodic, and the ensuing oscillations of the cytoplasmic Ca^{2+} concentration ($[Ca^{2+}]_i$) result in pulsatile insulin release (Gilon et al., 1993; Bergsten et al., 1994). In isolated β cells, the dominating $[Ca^{2+}]_i$ oscillation frequency is 0.1–0.5 min^{-1}, but faster (2–6 min^{-1}) oscillations and mixed patterns also occur, especially in β cells located in islets of Langerhans (Valdeolmillos et al., 1989; Liu et al., 1998). Glucose stimulates insulin secretion also at steps distal to the elevation of $[Ca^{2+}]_i$ (Henquin, 2000). The mechanisms underlying this effect are unclear, but may involve changes in the ATP/ADP ratio. Although glucose-induced $[Ca^{2+}]_i$ oscillations trigger pulsatile insulin release, secretion remains pulsatile also when $[Ca^{2+}]_i$ is stable (Westerlund et al., 1997). Thus, apart from Ca^{2+}, other factors controlling secretion can be expected to oscillate in β cells. There is evidence that metabolism oscillates in parallel with $[Ca^{2+}]_i$ in β cells. For example, $[Ca^{2+}]_i$ oscillations correlating with those of glucose and oxygen consumption, NAD(P)H and glucose-6-phosphate concentration, as well as the ATP/ADP ratio, have been recorded in isolated islets of Langerhans and suspensions of islet cells (Longo et al., 1991; Nilsson et al., 1996; Jung et al., 2000; Luciani et al., 2006).

Cyclic AMP (cAMP) is another critical messenger for insulin release (Hellman et al., 1974; Wollheim and Sharp, 1981; Schuit and Pipeleers, 1985; Prentki and Matschinsky, 1987), and the nucleotide potently enhances Ca^{2+} signals and exocytosis both via protein kinase A (PKA)-dependent and -independent mechanisms (Ämmälä et al., 1993; Renström et al., 1997; Takahashi et al., 1999; Eliasson et al., 2003; Dyachok and Gylfe, 2004; Seino and Shibasaki, 2005). Glucose was found to cause elevation of cAMP in β cells (Charles et al., 1973; Grill and Cerasi, 1973). However, since the reported effects were modest (Charles et al., 1973; Hellman et al., 1974; Schuit and Pipeleers, 1985), and cAMP alone is a poor trigger of insulin secretion (Hellman et al., 1974; Wollheim and Sharp, 1981; Prentki and Matschinsky, 1987), a view has emerged that cAMP is of minor importance for glucose-induced insulin secretion. Instead, cAMP is regarded to mediate the amplification of insulin secretion by glucagon and incretin hormones, such as glucagon-like peptide-1 (GLP-1). Glucose potently amplifies the hormone-induced elevations of cAMP, an effect proposed to be mediated by the elevation of $[Ca^{2+}]_i$ (Delmeire et al., 2003). In contrast to $[Ca^{2+}]_i$ signaling, which has been extensively characterized, little is known about the spatiotemporal kinetics of cAMP. Using a fluorescence resonance energy transfer biosensor, glucose was recently found to trigger concurrent cAMP and $[Ca^{2+}]_i$ elevation in individual MIN6 β cells (Landa et al., 2005). We recently developed an evanescent-wave microscopy technique for real-time recordings of the cAMP concentration beneath the plasma membrane ($[cAMP]_i$) of individual cells (Dyachok et al., 2006) and found that stimulation of insulin-secreting cells with GLP-1 triggers pronounced oscillations of $[cAMP]_i$ that were coordinated

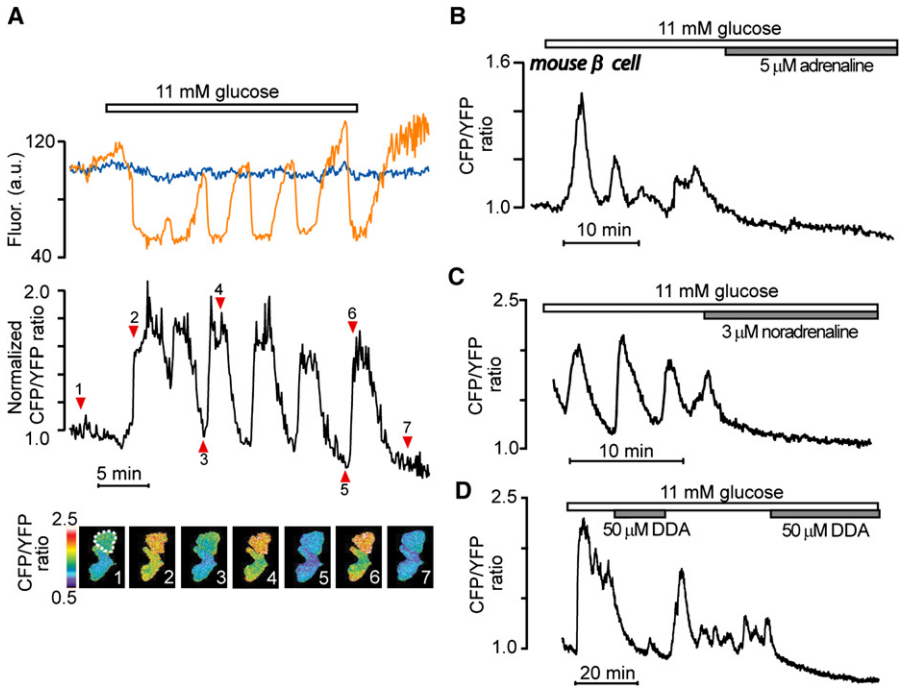

Figure 1. Glucose Triggers $[cAMP]_i$ Oscillations in β Cells

(A) Evanescent-wave microscopy recording of ΔRIIβ-CFP-CAAX (blue) and Cα-YFP (yellow) fluorescence from a MIN6 β cell during elevation of the glucose concentration from 3 to 11 mM. The prestimulatory CFP/YFP ratio was normalized to unity. Pseudocolor ratio images are from the time points indicated by numbered arrowheads, and the region of interest is encircled by a dashed line.

(B) Glucose-induced $[cAMP]_i$ oscillations in a single mouse pancreatic β cell. The response is inhibited by 5 μM adrenaline.

(C and D) Inhibition of $[cAMP]_i$ oscillations in MIN6 cells by 3 μM noradrenaline (C) and 50 μM 2′5′-dideoxyadenosine (DDA) (D).

with elevations of $[Ca^{2+}]_i$. Using this method in combination with single-cell recordings of insulin release, we now investigated the kinetics of glucose-induced $[cAMP]_i$ signaling in β cells and whether this messenger partakes in the dynamic pacing of insulin secretion.

RESULTS

Glucose Triggers Oscillations of $[cAMP]_i$

Mouse-derived MIN6 β cells were transfected with a fluorescent-translocation biosensor comprised of a truncated and membrane-anchored PKA regulatory subunit tagged with cyan-fluorescent protein (ΔRIIβ-CFP-CAAX), and a catalytic subunit labeled with yellow-fluorescent protein (Cα-YFP) (Dyachok et al., 2006). Holoenzyme dissociation caused by elevation of $[cAMP]_i$ results in translocation of Cα-YFP to the cytoplasm, recorded with evanescent-wave microscopy as selective loss of YFP fluorescence with rise of the CFP/YFP-fluorescence ratio (Figure 1A).

When the glucose concentration was raised from 3 to 11 mM, there was a temporary decrease of $[cAMP]_i$ (Δ ratio = 0.043 ± 0.006, $p < 0.001$, n = 28) followed after some delay (3.54 ± 0.23 min, n = 28) by a rapid rise ($t_{1/2}$ = 0.63 ± 0.17 min, n = 28) and pronounced oscillations (Figure 1A). The oscillatory pattern varied among cells with frequencies in the 0.07–1.8 min^{-1} range and amplitudes from 0.13 to 2.4 ratio units. The nadirs between oscillations often did not reach the baseline (Figures 1D, 2A, and 2B), but after lowering of the glucose concentration, the ratio quickly returned to the prestimulatory level (Figure 1A). Restimulation with the same glucose concentration resulted in a similar average response (100% ± 25% of first response, n = 11; data not shown). Oscillatory responses were also observed after elevation of the glucose concentration from 3 to 20 mM (n = 34, data not shown). Primary mouse pancreatic β cells infected with adenoviruses encoding the cAMP biosensor reacted similarly with pronounced $[cAMP]_i$ oscillations in response to glucose stimulation (n = 18; Figures 1B and 2C; frequencies 0.10–0.63 min^{-1}, amplitudes 0.09–0.98 ratio units). The glucose-induced $[cAMP]_i$ oscillations in mouse β cells were abolished by 5 μM adrenaline (n = 15, Figure 1B), consistent with α_2-adrenergic suppression of adenylyl cyclase activity in β cells (Schuit and Pipeleers, 1986). A similar effect was observed in MIN6 cells exposed to 3 μM adrenaline (n = 9, data not shown) or noradrenaline (n = 6; Figure 1C), or to 50 μM of the adenylyl cyclase inhibitor 2′,5′-dideoxyadenosine (DDA, n = 8; Figure 1D).

Ca^{2+} Amplifies, but Is Not Essential, for Glucose-Induced Oscillations of $[cAMP]_i$

Like primary β cells from rodents and humans (Hellman et al., 1994), most MIN6 cells respond to glucose with a small initial lowering of $[Ca^{2+}]_i$, followed by a pronounced increase with oscillations due to periodic depolarization and influx of Ca^{2+} through voltage-dependent channels (See Figure S1 in the Supplemental Data). Since the glucose-induced $[cAMP]_i$ response resembled that of $[Ca^{2+}]_i$, which has been proposed to play an important role in β cell generation and degradation of cAMP (Sharp,

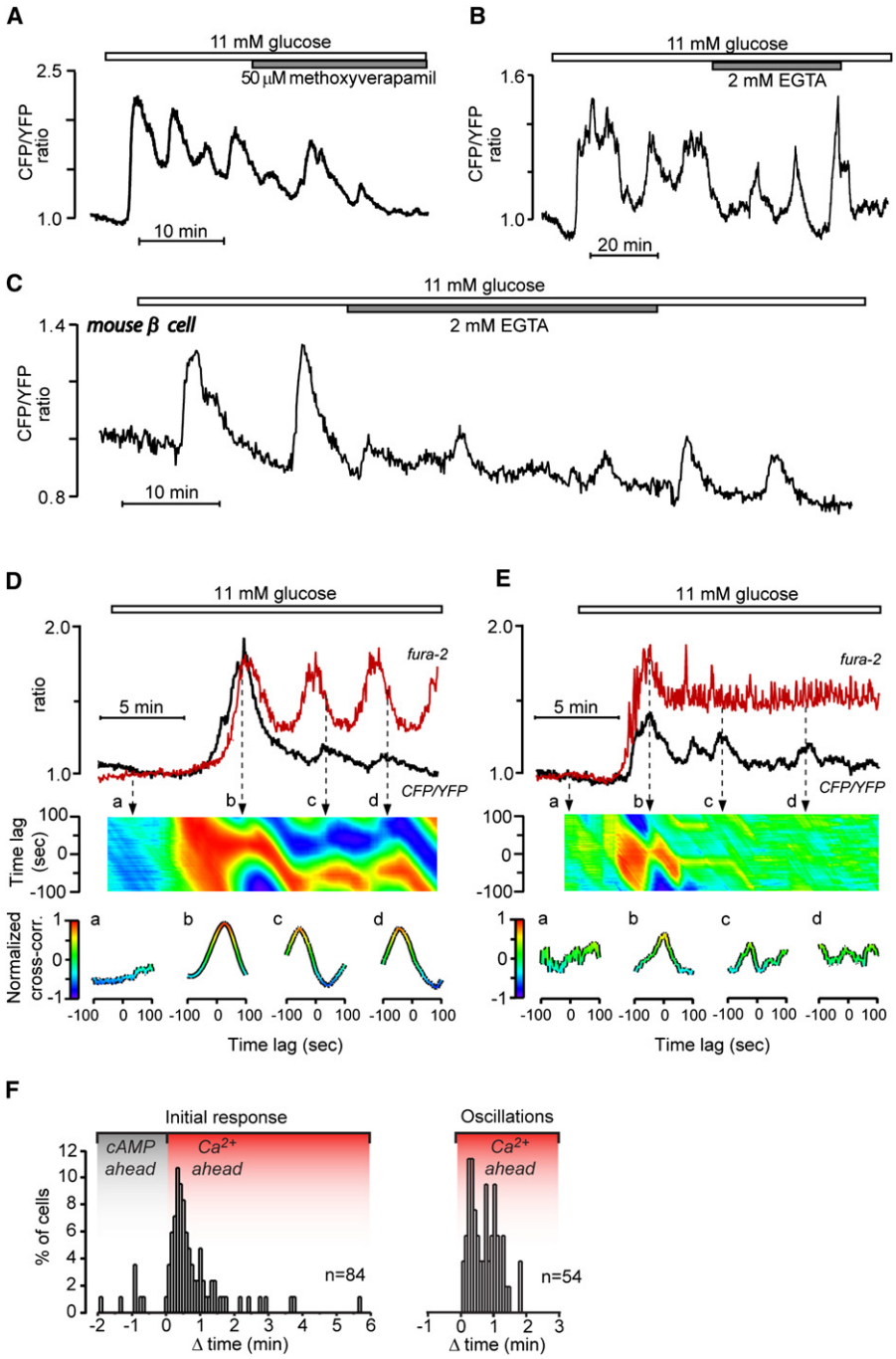

Figure 2. Glucose-Induced $[cAMP]_i$ Oscillations Are Amplified by Ca^{2+} but Are Not Tightly Linked to Changes in $[Ca^{2+}]_i$

(A and B) Evanescent-wave microscopy recordings of glucose-induced changes of $[cAMP]_i$ in MIN6 β cells when Ca^{2+} influx was prevented with 50 μM methoxyverapamil (A) or by Ca^{2+} removal and addition of 2 mM EGTA (B).

(C) Effect of Ca^{2+}-deficient medium on glucose-induced $[cAMP]_i$ oscillations in a single mouse pancreatic β cell.

(D and E) Simultaneous recording of $[cAMP]_i$ (black) and $[Ca^{2+}]_i$ (red) in fura-2-loaded MIN6 β cells during elevation of the glucose concentration from 3 to 11 mM. (D) shows that $[cAMP]_i$ increases before $[Ca^{2+}]_i$, during initial stimulation, and after $[Ca^{2+}]_i$ during subsequent oscillations. (E) shows that $[Ca^{2+}]_i$ rises before $[cAMP]_i$ during initial stimulation and that subsequent $[cAMP]_i$ oscillations occur without associated changes of $[Ca^{2+}]_i$. The data were subjected to sliding-window crosscorrelation analysis. Correlation was calculated from consecutive pairs of data segments of 100 s duration and shifted 2 s in time in relation to the previous segment. Two-dimensional crosscorrelograms (colored areas) were constructed from consecutive one-dimensional crosscorrelations with time on the x axis, the time lag of the correlation on the y axis, and the normalized crosscorrelation amplitude coded in color. Bottom traces show one-dimensional crosscorrelograms at the time points indicated by the vertical lines. For clarity, the crosscorrelation amplitude is shown both numerically on the y axis and using the same color code as in the two-dimensional presentation. It is apparent that there is a high correlation during the initial $[cAMP]_i$ and $[Ca^{2+}]_i$ elevations (panel D,

1979; Prentki and Matschinsky, 1987; Delmeire et al., 2003; Landa et al., 2005), we investigated the Ca^{2+} dependence of glucose-induced $[cAMP]_i$ signaling. Consistent with regulation being at least partially independent of Ca^{2+}, the glucose-induced $[cAMP]_i$ oscillations in MIN6 cells often persisted, albeit significantly suppressed, in the presence of the voltage-dependent Ca^{2+}-channel inhibitor methoxyverapamil (50 μM, average ratio 41% ± 6% of the control level with glucose alone, n = 9, $p < 0.001$; Figure 2A) or in Ca^{2+}-deficient medium containing 2 mM EGTA (ethyleneglycol-bis(β-aminoethyl)-N,N,N′,N′-tetraacetic acid) (24% ± 7% of control, n = 5, $p < 0.001$; Figure 2B). Also, in primary mouse β cells, the $[cAMP]_i$ oscillations were significantly suppressed—but not completely abolished—by Ca^{2+} removal (n = 6, average ratio 24% ± 8% of control; Figure 2C). Simultaneous measurements of $[cAMP]_i$ and $[Ca^{2+}]_i$ in transfected MIN6 cells loaded with the fluorescent indicator fura-2 demonstrated that $[cAMP]_i$ and $[Ca^{2+}]_i$ oscillations were synchronized (Figure 2D). The temporal relationship was somewhat variable, with $[cAMP]_i$ sometimes increasing before (8 out of 84 cells; Figures 2D and 2F) but more often after (76 of 84 cells, Figures 2E and 2F) the initial glucose-induced rise of $[Ca^{2+}]_i$. During subsequent oscillations, $[cAMP]_i$ always increased after $[Ca^{2+}]_i$ (Figures 2D and 2F) with a time difference of 40 ± 4 s (n = 54, range 2.5–103 s; Figure 2F) between half-maximal elevations. Interestingly, 38 out of 60 cells showed $[cAMP]_i$ oscillations without tightly associated changes in $[Ca^{2+}]_i$. Figure 2E shows a recording from a cell with slow oscillations of $[cAMP]_i$ without corresponding slow oscillatory changes in $[Ca^{2+}]_i$, although two of the $[cAMP]_i$ oscillations were preceded by brief $[Ca^{2+}]_i$ spikes. The temporal coordination and phase relationship between $[Ca^{2+}]_i$ and $[cAMP]_i$ signals were confirmed by crosscorrelation analysis (Figures 2D and 2E). To test if the dissociation between the cAMP and Ca^{2+} signals was due to the epifluorescence $[Ca^{2+}]_i$ measurements with fura-2 being performed in a larger cell volume than the evanescent-wave microscopy recordings of $[cAMP]_i$, we performed simultaneous evanescent-wave recordings of $[Ca^{2+}]_i$ and $[cAMP]_i$. To this end, the cells were transfected with a cAMP indicator based on a Cα-CFP construct and a ΔRIIβ-CAAX regulatory subunit lacking fluorescence tag to avoid spectral overlap with the Ca^{2+}-indicator Fura Red. With this approach the glucose-induced $[cAMP]_i$ elevation occurred before the initial rise of $[Ca^{2+}]_i$ in 4 of 10 cells (time difference: 6–81 s) and after $[Ca^{2+}]_i$ in the remaining 6 cells (time difference: 9–320 s, Figure S2). As in the fura-2 measurements, $[cAMP]_i$ always increased after $[Ca^{2+}]_i$ during subsequent oscillations (7–162 s, n = 8). Together, these findings indicate that Ca^{2+} amplifies but is not essential for glucose-induced rise of $[cAMP]_i$. The initial reduction of $[cAMP]_i$ may reflect lowering of $[Ca^{2+}]_i$ (Chow et al., 1995) below a permissive level for basal cAMP production.

cAMP Production Is Directly Stimulated by Cell Metabolism

There is evidence that β cell metabolism is oscillatory and that these oscillations may underlie those of $[Ca^{2+}]_i$ (Longo et al., 1991; Nilsson et al., 1996; Jung et al., 2000). We next aimed to clarify whether variations in metabolism are also involved in the generation of $[cAMP]_i$ oscillations. In MIN6 cells hyperpolarized with 250 μM of the K_{ATP} channel-opener diazoxide, elevation of glucose from 3 to 11 or 20 mM failed to raise $[cAMP]_i$. In contrast, when $[Ca^{2+}]_i$ was allowed to increase upon removal of diazoxide, there was a rapid and pronounced elevation of $[cAMP]_i$ (25% ± 6% increase of average ratio, n = 5, $p < 0.02$; Figure 3A). Depolarization with 30 mM K^+ in the presence of 3 mM glucose and 250 μM diazoxide caused a prompt but modest elevation of $[cAMP]_i$ (9.4% ± 1.3% increase of average ratio, n = 7, $p < 0.001$) that was reversed upon normalization of the K^+ concentration (Figure 3B). This response was much enhanced when the cells were restimulated in the presence of 11 mM glucose (2.5 ± 0.4-fold, n = 6, $p < 0.02$; Figure 3B). Likewise, when the glucose concentration was elevated from 3 to 11 mM during depolarization with 30 mM K^+ in the presence of diazoxide, there was a pronounced rise of $[cAMP]_i$ (2.1 ± 0.3-fold the response to depolarization alone, n = 11, $p < 0.01$), often with superimposed oscillations (Figure 3C; frequency = 0.19 ± 0.02 min^{-1}, n = 8). Similar data were obtained from mouse pancreatic β cells with a small K^+-induced elevation of $[cAMP]_i$ that was markedly enhanced by elevation of glucose from 3 to 11 mM in the presence of diazoxide (Figure 3D, n = 6). Under these depolarizing conditions, adrenaline (3–5 μM) immediately lowered $[cAMP]_i$ to baseline both in primary mouse β cells (Figure 3D) and clonal MIN6 cells (data not shown). This finding demonstrates that the inhibitory effect of adrenaline on cAMP production is not secondary to its hyperpolarizing action (Santana de Sa et al., 1983). We also tested the effect of α-ketoisokaproic acid (KIC), an insulin secretagogue that stimulates ATP production by β cell mitochondria (Lembert and Idahl, 1998). When added to depolarized MIN6 cells, 2 mM KIC induced a marked but transient increase in $[cAMP]_i$ (2.6 ± 0.6-fold the response to depolarization alone, n = 6, $p < 0.05$; Figure 3E). These effects of glucose and KIC on $[cAMP]_i$ were not paralleled by increases of $[Ca^{2+}]_i$. Instead, elevation of glucose or addition of KIC induced transient lowering of $[Ca^{2+}]_i$ from the levels obtained by K^+ depolarization (Figure S1). Consistent with mitochondrial metabolism being essential for the nutrient-induced elevation of $[cAMP]_i$, the effect of glucose was promptly reversed by 0.1–1 μM of the uncoupler FCCP (carbonylcyanide-p-trifluoromethoxyphenylhydrazone, n = 5; Figure 3F). Our data thus confirm observations that elevation of $[Ca^{2+}]_i$ is sufficient to trigger rise of $[cAMP]_i$ in β cells (Landa et al., 2005). However, we also show that stimulation of metabolism is a potent trigger of cAMP production in β cells with elevated $[Ca^{2+}]_i$.

To test whether ATP, the substrate for adenylyl cyclases, may be the mediator of the metabolically stimulated adenylyl cyclase activity, we investigated the effect of a sudden suppression of cellular ATP consumption by ouabain inhibition of the Na^+/K^+-ATPase. Ouabain has previously been found to suppress K_{ATP} channel activity in β cells by increasing the ATP concentration beneath the plasma membrane (Grapengiesser et al., 1993).

line b; panel E, line b) and during subsequent oscillations in panel D (lines c and d). In contrast, correlation is low during the prestimulatory phase (panel D, line a; panel E, line a) and when $[cAMP]_i$ shows slow oscillations while $[Ca^{2+}]_i$ does not (panel E, lines c and d).
(F) Distribution of time differences between the half-maximal rise of $[Ca^{2+}]_i$ and $[cAMP]_i$ during the initial glucose response and subsequent oscillations shown in histograms with 5 s intervals.

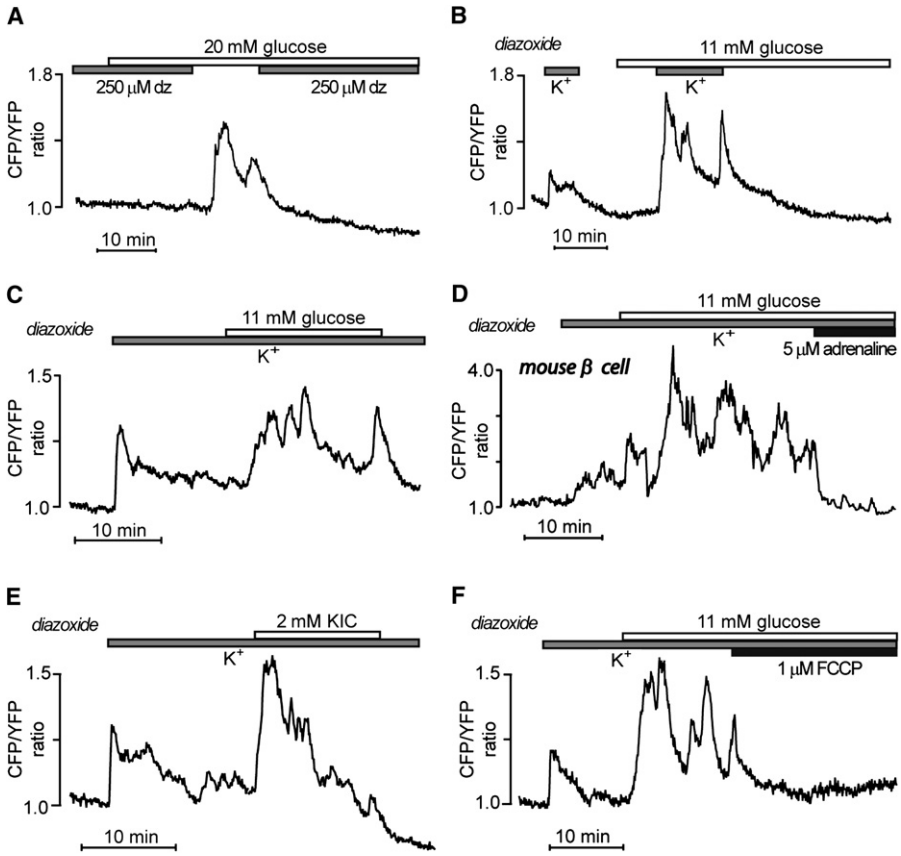

Figure 3. Stimulation of Metabolism Triggers cAMP Formation in the Presence of Elevated $[Ca^{2+}]_i$

(A) Elevation of the glucose concentration from 3 to 20 mM fails to raise $[cAMP]_i$ in MIN6 β cells hyperpolarized with diazoxide (dz).

(B) $[cAMP]_i$ elevation triggered by membrane depolarization with 30 mM K^+ in the presence of 250 μM diazoxide is enhanced by increase of the glucose concentration from 3 to 11 mM.

(C and D) Elevation of the glucose concentration from 3 to 11 mM triggers pronounced $[cAMP]_i$ elevation with oscillations in MIN6 cells (C), and mouse pancreatic β cells (D) depolarized with 30 mM K^+ in the presence of 250 μM diazoxide. This response is counteracted by 5 μM adrenaline (D).

(E) Stimulation of $[cAMP]_i$ elevation by 2 mM KIC in depolarized MIN6 β cells.

(F) The $[cAMP]_i$ elevation in depolarized MIN6 cells exposed to 11 mM glucose is suppressed by 1 μM of the mitochondrial uncoupler FCCP.

When added to MIN6 cells depolarized with KCl in the presence of diazoxide, ouabain was now found to raise $[cAMP]_i$ (9.0% ± 1.7% increase of the average ratio, n = 6, $p < 0.01$) without apparent effects on $[Ca^{2+}]_i$ (Figures 4A and 4B). More direct support for the involvement of ATP as a regulator of cAMP production came from experiments on MIN6 cells permeabilized with staphylococcal α-toxin. As shown in Figure 4C, elevation of the ATP concentration from 1 to 4 mM caused a significant and reversible elevation of $[cAMP]_i$ (7.5% ± 1.7% increase of average ratio, n = 8, $p < 0.01$), which was further increased by 16% ± 4% (n = 4, $p < 0.05$) after addition of 50 μM forskolin and 100 μM of 3-isobutyl-1-methylxanthine (IBMX). These relatively poor cAMP responses are likely due to washout of cAMP from the permeabilized cells.

$[cAMP]_i$ Oscillations Regulate Pulsatile Insulin Release

To investigate whether the glucose-induced oscillations of $[cAMP]_i$ are important for the kinetics of insulin release, the time course of secretion was recorded from individual cells by real-time monitoring of the autocrine activation of insulin receptors. We recently found that insulin release from isolated β cells results in strong autocrine activation of phosphoinositide 3-OH-kinase (PI3-kinase), and that the PI3-kinase-induced formation of phosphatidylinositol-3,4,5-trisphosphate (PIP_3) can be monitored with evanescent-wave microscopy as membrane translocation of fluorescent protein-tagged PIP_3-binding protein domains (Idevall-Hagren and Tengholm, 2006). The validity of this method was further substantiated by relating the formation of PIP_3 to evanescent-wave microscopy imaging of the plasma-membrane insertion of fluorescence-tagged insulin secretory vesicles. PIP_3 was measured with the CFP-tagged pleckstrin homology domain (PH domain) from protein kinase B/Akt (Haugh et al., 2000), and granules were monitored with YFP fused to the vesicle membrane protein 2 (VAMP2). The fluorescence-tagged VAMP2 approach has been extensively used to monitor exocytosis in different types of cells, including insulin-secreting cells (Tsuboi and Rutter, 2003). MIN6 cells expressing the reporter constructs reacted to membrane depolarization (30 mM KCl) with prompt incorporation of VAMP2-YFP in the plasma membrane (26% ± 4% increase of overall YFP fluorescence in the

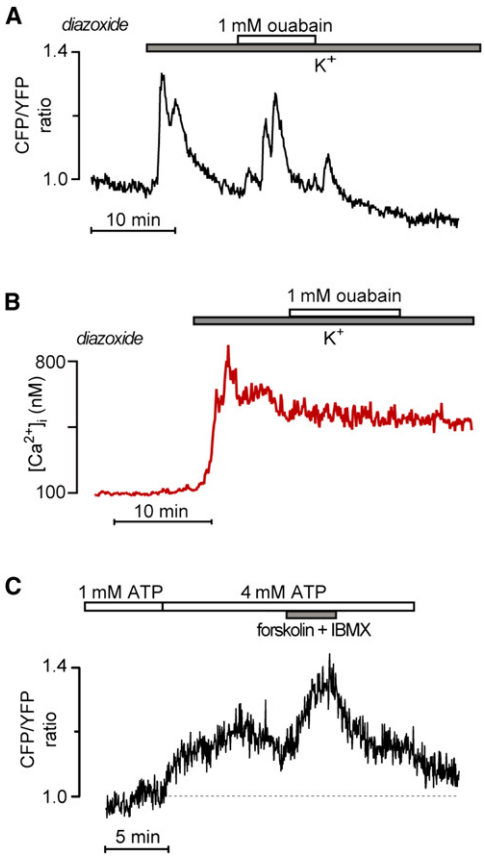

Figure 4. Increase of $[cAMP]_i$ by Elevation of ATP Concentration

(A) Inhibition of the ATP-consuming Na^+/K^+-ATPase with 1 mM ouabain triggers elevation of $[cAMP]_i$ in MIN6 β cells depolarized with 30 mM K^+ in the presence of 250 μM diazoxide.

(B) The same treatment had no effect on $[Ca^{2+}]_i$ recorded with epifluorescence microscopy in a single MIN6 β cell loaded with fura-2.

(C) Stimulation of cAMP formation by elevation of the ATP concentration from 1 to 4 mM and addition of 50 μM forskolin and 100 μM IBMX in a MIN6 β cell permeabilized with α-toxin.

membrane), followed after a 12 ± 3 s delay by elevation of PIP_3 (59% ± 7% rise of CFP fluorescence, n = 14; Figure 5A). Similar responses were seen when repeating the depolarizations after 5–10 min delays. This finding is consistent with a tight link between exocytosis of insulin granules and autocrine activation of insulin receptors. In subsequent experiments, we transfected cells with the "general receptor for phosphoinositides-1" fused to a construct with four copies of GFP (GFP_4-GRP1). Compared to previously used constructs, this biosensor provides improved response by its brighter fluorescence and nuclear exclusion. Elevation of the glucose concentration from 3 to 11 mM triggered a rise of evanescent wave-excited GFP_4-GRP1 fluorescence (161% ± 14%, n = 39) with pronounced oscillations from a level slightly above baseline (frequency = 0.22 ± 0.01 min^{-1}; Figures 5B–5D, and 6). Inhibition of the insulin receptor tyrosine kinase with 200 μM hydroxy-2-naphthalenylmethylphosphonic acid tris-acetoxymethyl ester ($HNMPA\text{-}AM_3$, n = 7), or of PI3-kinase with 100 μM LY294002 (n = 10), suppressed the fluorescence signal to the baseline (Figures 5B and 5C). Moreover, insulin-receptor antibodies prevented the glucose-induced GFP_4-GRP1 fluorescence response (Figures 5D and 5E). When insulin secretion was inhibited by preventing voltage-dependent Ca^{2+} influx with methoxyverapamil (n = 15) or Ca^{2+}-deficient medium (n = 21), there was also an immediate reversal of the GFP_4-GRP1 signal to the prestimulatory level (Figures 6A and 6B). In contrast, elevation of $[cAMP]_i$ by addition of 100 μM of IBMX or 10 μM of the adenylyl cyclase activator forskolin induced a prompt rise of the PIP_3 signal followed by stable elevation or oscillations, often with increased amplitude (Figures 6C and 6E). Time-average PIP_3 elevation was markedly increased in the presence of IBMX or forskolin (Figure 6E), reinforcing the importance of cAMP for controlling the magnitude of insulin secretion. Consistent with a key role of $[cAMP]_i$ oscillations for pulsatile insulin release, the adenylyl cyclase inhibitor DDA (50 μM) markedly suppressed or even abolished the glucose-induced oscillations of PIP_3 (average PIP_3 elevation = 45% ± 5% of control, n = 30, $p < 0.001$; Figures 6D and 6E), without effect on those of $[Ca^{2+}]_i$ (Figure S3). Control experiments showed that changes of $[cAMP]_i$ had little effects on the insulin-induced PI3-kinase activity (Figure S3).

For simultaneous measurements of $[cAMP]_i$ and PIP_3, we used alternative biosensors that could be combined without spectral interference. $[cAMP]_i$ measurements were made with the PKA catalytic Cα-YFP construct combined with the ΔRIIβ-CAAX regulatory subunit lacking fluorescent-protein tag. This allowed PIP_3 to be measured with CFP fused to the PH domain from protein kinase B/Akt. The recordings revealed coordinated oscillations of $[cAMP]_i$ and insulin secretion (Figure 6F). Each oscillation of PIP_3 was preceded by rise of $[cAMP]_i$ by 16 ± 4 s (n = 37, Figure 6G), and there was a linear correlation between the amplitudes of $[cAMP]_i$ and PIP_3 oscillations (r = 0.687–0.998, $p < 0.01$, n = 9 cells; Figure 6H). Together, these findings indicate that glucose-induced pulsatile insulin release is determined by coordinated oscillations of $[Ca^{2+}]_i$ and $[cAMP]_i$.

DISCUSSION

cAMP is a key regulator of exocytosis in many cells and has long been known as a potent amplifier of insulin secretion (Hellman et al., 1974; Sharp, 1979; Prentki and Matschinsky, 1987). Nevertheless, it has not been clear to what extent changes in cAMP take part in glucose-induced insulin secretion from pancreatic β cells. In the present study, we took advantage of a new technique for single-cell measurements of the cAMP concentration beneath the plasma membrane (Dyachok et al., 2006) and show that glucose alone triggers a marked elevation of $[cAMP]_i$ with oscillations in both clonal insulin-secreting MIN6 cells and primary mouse pancreatic β cells. Moreover, coordination of glucose-induced $[cAMP]_i$ and $[Ca^{2+}]_i$ oscillations was required for optimal amplitude of pulsatile insulin release from single β cells. The effects of glucose on $[cAMP]_i$ may have been underestimated in previous studies using traditional biochemical detection of cAMP (Charles et al., 1973; Hellman et al., 1974) (Schuit and Pipeleers, 1985) because the time-average cAMP concentration is lower than the peaks reached during oscillations. Another possibility is that the cAMP concentration is lower in the bulk cytoplasm than in the vicinity of the adenylyl cyclases beneath the plasma membrane. The absence of cAMP oscillations in a recent imaging study of MIN6 cells stimulated with glucose alone (Landa

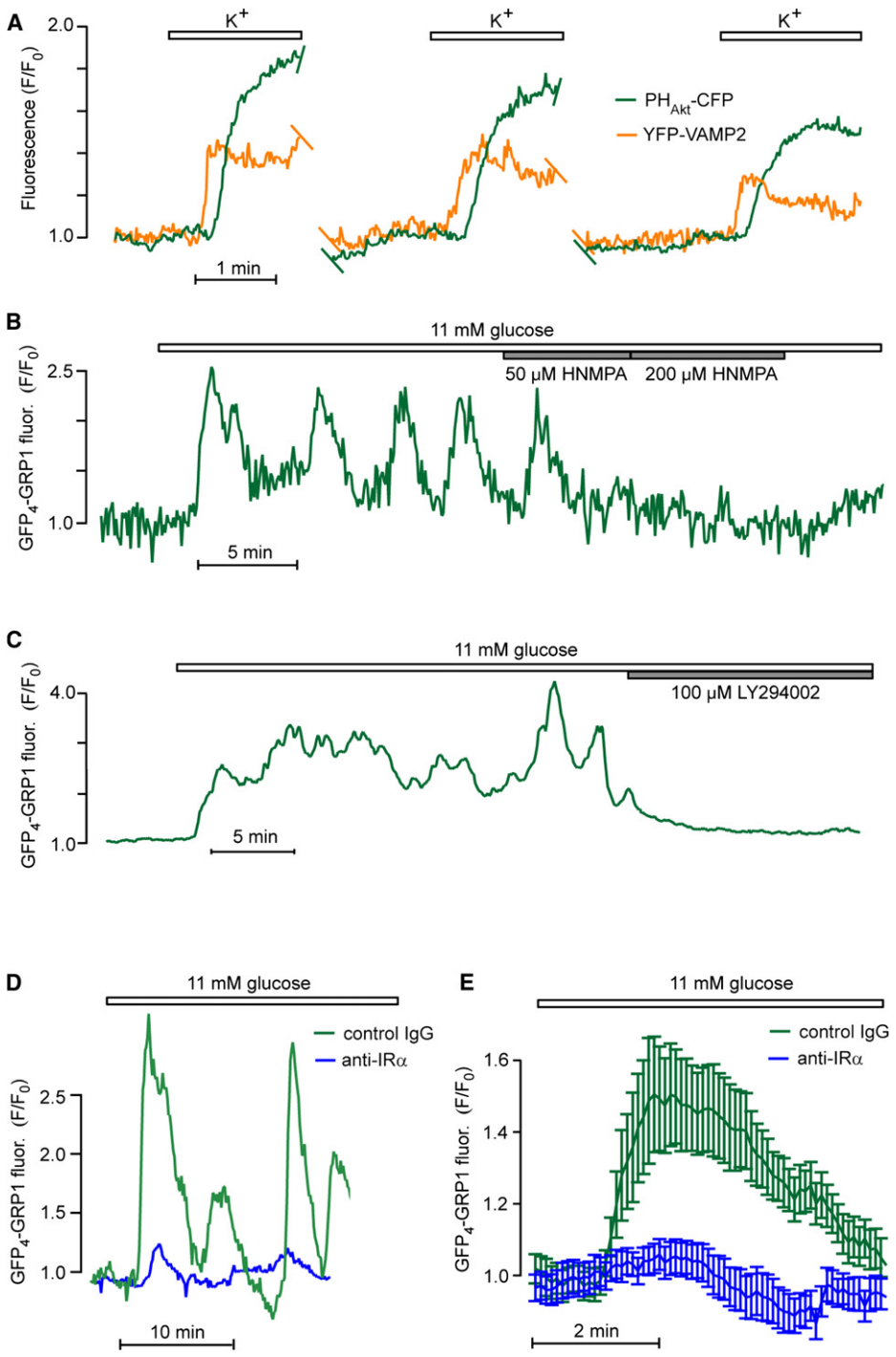

Figure 5. Glucose-Induced Formation of Membrane PIP_3 Depends on Activation of Insulin Receptors and PI3-Kinase

(A) Simultaneous evanescent-wave microscopy recording of the PIP_3 concentration and insulin granule-membrane protein insertion into the plasma membrane in MIN6 cells. The CFP-tagged PH domain from Akt was used for PIP_3 measurements and YFP-tagged VAMP2 as granule marker. The traces show the responses to three consecutive 90 s depolarizations with 30 mM KCl. Image pairs were acquired every 0.9 s. To minimize exposure to the excitation light, recordings were interrupted during 10 and 5 min, respectively, between the stimulations. Membrane depolarization induces prompt VAMP-YFP membrane insertion, which precedes the elevation of PIP_3.

(B and C) Evanescent-wave microscopy recording of plasma membrane PIP_3 concentration in single MIN6 β cells expressing the "general receptor for phosphoinositides-1" fused to a tandem construct with four GFP molecules (GFP_4-GRP1). Elevation of the glucose concentration from 3 to 11 mM triggers pronounced translocation of the reporter to the plasma membrane (increase of fluorescence), reflecting insulin secretion with autocrine activation of insulin receptors. The response is completely suppressed by 200 μM of the insulin receptor tyrosine kinase inhibitor HNMPA (B) or by 100 μM of the PI3-kinase inhibitor LY294002 (C).

(D) Glucose-induced PIP_3 responses of individual MIN6 β cells preincubated 30 min in the presence of anti-insulin receptor (anti-IRα) or control IgG antibodies.

(E) Averages ± SEM. for the initial glucose-induced PIP_3 responses (n = 14 [anti-IRα] and 16 [control IgG]).

et al., 2005) may be due to the use of a lower-affinity biosensor reporting cAMP concentration in the entire cytoplasm.

The glucose-induced changes in $[cAMP]_i$ resembled those of $[Ca^{2+}]_i$ with a small intitial lowering, followed by a pronounced rise and slow oscillations with a period of 2–10 min. β cells express Ca^{2+}-calmodulin-sensitive adenylyl cyclases (Valverde et al., 1979; Delmeire et al., 2003) and phosphodiesterases (Pyne and Furman, 2003; Landa et al., 2005), and changes in $[Ca^{2+}]_i$ can therefore be expected to influence cAMP formation and degradation. Activation of G_s-coupled hormone receptors (Dyachok et al., 2006) or depolarization with tetraethylammonium (Landa et al., 2005) have previously been found to induce cAMP oscillations in clonal β cells in a $[Ca^{2+}]_i$-dependent manner. cAMP oscillations secondary to elevations of $[Ca^{2+}]_i$ have also been reported in other types of cells (Gorbunova and Spitzer, 2002; Dunn et al., 2006; Willoughby and Cooper, 2006). The phase relationship between Ca^{2+} and cAMP signals in insulin-secreting cells seems to differ depending on the conditions. Whereas cells stimulated with GLP-1 showed synchronous oscillations of $[cAMP]_i$ and $[Ca^{2+}]_i$ (Dyachok et al., 2006), tetraethylammonium-induced elevations of $[Ca^{2+}]_i$ were associated with decreases of cAMP (Landa et al., 2005), interpreted as periodic activation of the Ca^{2+}-sensitive PDE1 family of phosphodiesterases. The present data show that glucose-induced $[cAMP]_i$ oscillations were enhanced by Ca^{2+} and coordinated with $[Ca^{2+}]_i$ oscillations. However, the glucose-induced $[cAMP]_i$ oscillations are not directly driven by the changes in $[Ca^{2+}]_i$. For example, $[cAMP]_i$ oscillations were not completely prevented even after 30 min in Ca^{2+}-deficient medium. Moreover, in some cells the initial rise of $[cAMP]_i$ preceded that of $[Ca^{2+}]_i$, and $[cAMP]_i$ oscillations occurred also under conditions when $[Ca^{2+}]_i$ showed a stable elevation. The observations that the glucose-induced $[cAMP]_i$ signal is abolished by membrane hyperpolarization with diazoxide but incompletely suppressed by preventing Ca^{2+} influx may possibly indicate that β cells, like cerebellar granule cells (Reddy et al., 1995), express depolarization-sensitive adenylyl cyclases.

The present study demonstrates that cell metabolism is a strong stimulus for cAMP production when $[Ca^{2+}]_i$ is elevated. Considering the many putative regulatory influences on adenylyl cyclases and phosphodiesterases, $[cAMP]_i$ is likely to be under dynamic control by multiple factors, some of which may be directly linked to cell metabolism. ATP seems to be a reasonable candidate for regulating adenylyl cyclase, since ATP is the substrate for this enzyme. Although indirect regulation or other metabolites cannot be excluded, the observations that cAMP formation was stimulated by acute suppression of ATP consumption with ouabain or by exposing permeabilized cells to millimolar ATP concentrations underscore the importance of ATP as a regulator of cAMP production. It may be argued that cytoplasmic ATP varies relatively little and that physiological concentrations of the nucleotide are higher than the K_m of mouse islet adenylyl cyclases, which have been estimated to be 0.32 mM in vitro (Davis and Lazarus, 1972). However, also the ATP-sensitive K^+ channels (Tarasov et al., 2006; Schulze et al., 2007) and the sarco(endo)plasmic reticulum Ca^{2+} ATPases (SERCAs) (Tengholm et al., 1999) are regulated by cytoplasmic ATP although the in vitro sensitivities to ATP are in the micromolar range. In the case of the K_{ATP} channel, the ATP sensitivity is reduced by ADP, which can be formed by local ATP hydrolysis (Tarasov et al., 2006) or phosphotransfer reactions (Schulze et al., 2007). Metabolism and the ATP/ADP ratio are known to undergo periodic variations in β cells (Longo et al., 1991; Nilsson et al., 1996; Jung et al., 2000; Luciani et al., 2006). Our results are consistent with the idea that such variations underlie the glucose-induced $[cAMP]_i$ oscillations.

cAMP in the submembrane space has important effects on ion channels and exocytosis of insulin granules (Ämmälä et al., 1993; Renström et al., 1997; Dyachok and Gylfe, 2004; Seino and Shibasaki, 2005). Indeed, our results demonstrate that $[cAMP]_i$ oscillations are critical for the magnitude of pulsatile insulin secretion. Direct stimulation of cAMP formation by submembrane ATP may explain the postpriming effects of ATP on exocytosis, which has been reported to involve activation of PKA (Takahashi et al., 1999). Glucose-induced generation of cAMP in β cells potentiates insulin secretion by sensitizing the exocytosis machinery, since inhibition of $[cAMP]_i$ oscillations markedly suppressed pulsatile insulin secretion without affecting the underlying $[Ca^{2+}]_i$ oscillations. The interplay between Ca^{2+}, ATP, and cAMP may thus contribute both to the triggering and amplifying pathways of insulin secretion (Henquin, 2000) and help to explain how insulin secretion from isolated islets can be pulsatile at stable $[Ca^{2+}]_i$ elevation (Westerlund et al., 1997). The direct link between cell metabolism and a signaling cascade of importance for insulin secretion, cell growth, differentiation, and survival has implications for understanding β cell dysfunction with loss of pulsatile insulin release in type 2 diabetes (Lang et al., 1981). Impaired glucose-induced cAMP formation has been reported in islets from diabetic animal models with reduced insulin secretion (Rabinovitch et al., 1976; Dachicourt et al., 1996), and cAMP-elevating agents have been found to ameliorate β cell function in diabetes (Abdel-Halim et al., 1996; Dachicourt et al., 1996). A direct coupling of metabolism to the ubiquitous cAMP-signaling cascade may have significance in many types of cells, controlling processes like gene transcription, cytoskeletal dynamics, cell adhesion, junction formation, ion fluxes, and exocytosis.

EXPERIMENTAL PROCEDURES

Materials

Adrenaline, noradrenaline, DDA, KIC, EGTA, HEPES, IBMX, insulin, HNMPA-AM_3, LY294002, ouabain, and FCCP were from Sigma. Diazoxide, methoxyverapamil, and forskolin were kind gifts from Schering-Plough, Knoll AG (Germany), and Aventis (Sweden), respectively. Insulin-receptor antibody (sc-710) and control IgG (sc-2027) were from Santa Cruz Biotechnology. The plasmids encoding the cAMP biosensor were created as previously described (Dyachok et al., 2006). To enable simultaneous measurements of $[cAMP]_i$ and PIP_3 or $[Ca^{2+}]_i$, we prepared a modified cAMP probe with the PKA regulatory subunit lacking the CFP tag and another one in which the YFP label of the catalytic subunit was replaced with CFP. The GFP_4-GRP1 construct was generated by ligating the full-length GRP1 protein in frame with four copies of GFP. The plasmids containing the CFP-tagged PH domain from Akt and YFP-tagged VAMP2 were originally from Professor Tobias Meyer, Stanford University.

Construction of Recombinant Adenoviruses

Recombinant adenovirus vectors expressing the cAMP-biosensor subunits under the transcriptional control of a tetracycline-regulatable promoter were created in several steps. First, ΔRIIβ-CFP-CAAX and Cα-YFP cDNA were PCR amplified with primers containing BclI and BamHI restriction sites. The products were ligated into the pShuttleTetTripLac-BamHI transfer vector (Berenjian and Akusjärvi, 2006). The resulting pShuttleTetTripLac-ΔRIIβ-CFP-CAAX

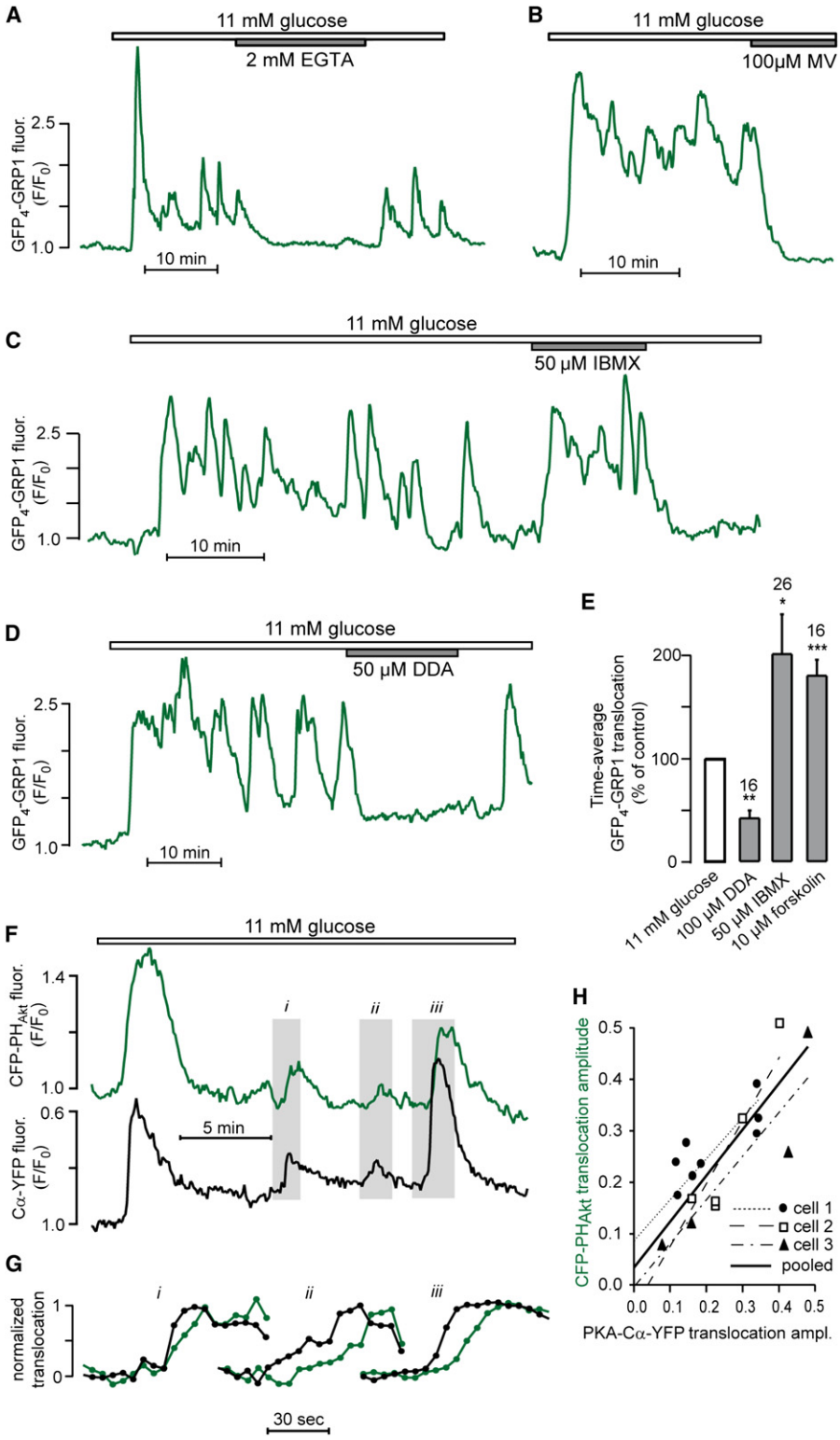

Figure 6. Glucose-Induced $[cAMP]_i$ Oscillations Regulate Pulsatile Insulin Release

(A and B) Glucose-induced pulsatile insulin secretion recorded with the PIP_3 biosensor GFP_4-GRP1. Secretion is inhibited by Ca^{2+} removal and addition of EGTA (A) as well as by 100 μM of the voltage-dependent Ca^{2+}-channel inhibitor methoxyverapamil (MV) (B).

(C) Elevation of $[cAMP]_i$ with the phosphodiesterase inhibitor IBMX amplifies insulin release.

(D) Pulsatile insulin secretion is suppressed by inhibition of adenylyl cyclases with 2′5′-dideoxyadenosine (DDA).

and pShuttleTetTripLac-Cα-YFP transfer vectors were linearized with PmeI and transformed into electrocompetent BJ5183 *E. coli* containing the plasmid pAd-Tet-ON. This plasmid contains the full-length adenovirus genome (Ad5) with deleted E1 and E3 regions (Berenjian and Akusjärvi, 2006). The desired recombinant adenovirus constructs were generated by overlap recombination (He et al., 1998), and recombinants were selected with kanamycin and screened by restriction enzyme analysis. The resulting constructions pAd-Tet-ON-ΔRIIβ-CFP-CAAX and pAd-Tet-ON-Cα-YFP were cleaved with PacI to expose its inverted-terminal repeats and subsequently transfected into 293-LacI cells (Edholm et al., 2001) using FUGENE 6 (Amersham Biosciences, Uppsala, Sweden) to make recombinant viruses. The cells were harvested 7–10 days posttransfection, freeze thawed to release virus particles, and resuspended in PBS with 1 mM $MgCl_2$ for reinfection. After three rounds of reinfection, high-titer virus stocks were produced in twelve 15 cm plates of 293-LacI cells infected with the recombinant viruses as previously described (Molin and Akusjärvi, 2000). Two to three days postinfection, when a clear cytopathic effect was visible, the cells were harvested by low-speed centrifugation and resuspended in 2 ml 0.1 M Tris-HCl (pH 8.0), followed by lysis with 0.1 volumes of 5% Na-deoxycholate for 30 min on ice. The cell lysates were subsequently sonicated on ice and viruses purified by CsCl-gradient centrifugation. Virus bands were collected and dialyzed against 100 volumes of PBS containing 1 mM $CaCl_2$, 1 mM $MgCl_2$, and 10% glycerol, using a Slide-A-Lyzer Cassette (Pierce, Rockford, IL). Virus titers were determined by counting fluorescent forming units (FFU) (Philipson, 1961) using a monoclonal antibody directed against the adenovirus-hexon protein (Sigma) and an FITC (fluorescein isothiocyanate)-conjugated secondary antibody (Sigma). Construction of the AdCMVrtTA virus containing the tetracycline-regulated transcriptional coactivator has been described previously (Molin et al., 1998).

Islet Isolation, Cell Culture, and Transfection

Insulin-secreting MIN6 β cells (passage 17–30; Miyazaki et al., 1990) were cultured as previously described (Idevall-Hagren and Tengholm, 2006). Transient transfection was performed with 2 μg plasmid DNA and 5 μg Lipofectamine 2000 (Invitrogen) in 1 ml DMEM for 4 hr followed by washing and further culture in DMEM for 12–24 hr. Islets were isolated from the pancreata of C57Bl/6 mice with the aid of collagenase. All procedures were approved by a local ethical committee on animal experiments. Single cells were prepared by shaking the islets in a Ca^{2+}-deficient medium. After resuspension in RPMI 1640 medium supplemented with 10% fetal calf serum, 100 IU/ml penicillin, and 100 μg/ml streptomycin, the cells were allowed to attach to the center of round coverslips during 2–5 days of culture at 37°C in an atmosphere of 5% CO_2 in humidified air. The islet cells were infected with viruses using a multiplicity of infection of 60 FFU/cell. After a 1 hr incubation at 37°C in culture medium, the inoculum was removed and the cells washed twice, followed by further culture in complete medium supplemented with 4 μM doxycycline for 24 hr. Before experiments, the cells were transferred to a buffer containing 125 mM NaCl, 4.8 mM KCl, 1.3 mM $CaCl_2$, 1.2 mM $MgCl_2$, and 25 mM HEPES (with pH adjusted to 7.40 with NaOH) and incubated for 30 min at 37°C. For $[Ca^{2+}]_i$ measurements, the cells were preincubated in the presence of 1–10 μM of the acetoxymethyl esters of the fluorescent Ca^{2+} indicators fura-2 (AnaSpec, Inc., San José, CA) or Fura Red (Invitrogen Molecular Probes). Primary mouse β cells were identified based on their large size and low nuclear/cytoplasmic ratio as well as their negative cAMP response to adrenaline.

Cell Permeabilization

Where indicated, the cells were permeabilized with α-toxin from *Staphylococcus aureus* (PhPlate Stockholm, Stockholm, Sweden). Before permeabilization, the cells were superfused with an intracellular-like medium containing 140 mM KCl, 6 mM NaCl, 0.1 mM EGTA, and 10 mM HEPES (with pH adjusted to 7.00 with KOH). Temporarily interrupting the perifusion, 5 μl α-toxin (0.46 mg/ml) were added directly into the 50 μl superfusion chamber. After permeabilization, 1–4 mM MgATP were added to the medium, and the concentrations of free Mg^{2+} and Ca^{2+} were maintained at 1 mM and 350 nM, respectively.

Fluorescence Microscopy

Plasma membrane association of the fluorescent protein-tagged PKA subunits VAMP2 and PIP_3-binding proteins were measured using a dual-wavelength evanescent-wave microscopy setup built around an E600FN upright microscope (Nikon, Kanagawa, Japan). A helium-cadmium laser (Kimmon, Tokyo, Japan) provided 442 nm light for excitation of CFP, and the 488 and 514 nm lines of an argon laser (Creative Laser Production, Munich, Germany) were used to excite GFP and YFP, respectively. The output from the lasers was controlled by a filter wheel equipped with an electronic shutter (Sutter Instruments, Novato, CA). The merged laser beam was homogenized and expanded by a rotating light-shaping diffuser (Physical Optics Corporation, Torrance, CA) and refocused through a modified quartz dove prism (Axicon, Minsk, Belarus) at an angle of 70° to achieve total internal reflection. The coverslips with the attached cells were used as exchangeable bottoms of an open 50 μl chamber and superfused with buffer at a rate of 0.3 ml/min. The chamber was mounted on the custom-built stage of the microscope such that the coverslip was maintained in contact with the dove prism by a layer of immersion oil. Regular "wide-field" excitation of fura-2 at 340 and 380 nm was achieved via an epifluorescence illuminator connected through a 3 mm diameter liquid-light guide to an Optoscan monochromator (Cairn Research, Ltd., Faversham, UK) equipped with a 150 W xenon-arc lamp. Regardless of the mode of illumination, fluorescence was collected through 40 × 0.8 NA or 60 × 1.0 NA water-immersion objectives (Nikon) and detected with a back-illuminated EMCCD camera (DU-887, Andor Technology, Belfast, Northern Ireland) under MetaFluor Molecular Devices Corporation, Downington, PA) software control. Emission wavelengths were selected with interference filters (525 nm/25 nm half-bandwidth for GFP, 485/25 nm for CFP, 560/40 nm for YFP, and 510/40 nm for fura-2) mounted in a filter wheel (Sutter Instruments). Images were acquired every 2–5 s using exposure times in the 70–200 ms range. Separate $[Ca^{2+}]_i$ recordings were performed with a regular imaging system as previously described (Dyachok and Gylfe, 2004).

Data and Statistical Analysis

Image analysis was made using the MetaFluor or ImageJ (W. S. Rasband, National Institute of Health, http://rsb.info.nih.gov/ij) softwares. The cAMP concentration was expressed as the ratio of CFP over YFP fluorescence after background subtraction. To compensate for the variability in expression levels, the basal ratio was normalized to unity. Response magnitudes were calculated from time-average data obtained before and during the stimulation period. $[Ca^{2+}]_i$ recorded with fura-2 is expressed either as 340/380 nm fluorescence-excitation ratio or as calibrated Ca^{2+} concentrations (Grynkiewicz et al., 1985). Fluorescence intensities were otherwise expressed in relation to initial fluorescence after subtraction of background (F/F_0). Data are presented as means ± SEM. Statistical comparisons were assessed with Student's t test.

SUPPLEMENTAL DATA

Supplemental data include three figures and can be found online at http://www.cellmetabolism.org/cgi/content/full/8/1/26/DC1/.

(E) Effect of cAMP-modulating agents on time-average GFP_4-GRP1 translocation. Means ± SEM. The number above each bar refers to the number of cells examined. *, $p < 0.02$; **, $p < 0.01$; ***, $p < 0.001$; Student's t test.
(F) Simultaneous recording of PIP_3 and $[cAMP]_i$ as CFP-PH_{Akt} and Cα-YFP translocation, respectively, demonstrates coordinated oscillations of $[cAMP]_i$ and insulin secretion.
(G) Time expansions and amplitude normalizations of the regions shaded in (F) show that elevations of $[cAMP]_i$ precede PIP_3 formation.
(H) Linear correlation between $[cAMP]_i$ and PIP_3 oscillation amplitudes. Scatter plots and regression lines for data from three individual cells and from the pooled data set.

ACKNOWLEDGMENTS

We thank Mrs. Heléne Dansk for preparation of mouse β cells, Dr. E-ri Sol for help with virus purification, and Professor Nils Welsh for sharing his virus lab facilities. This study was supported by grants from Åke Wiberg's Foundation, Carl Trygger's Foundation for Scientific Research, the European Foundation for the Study of Diabetes/MSD, the Family Ernfors Foundation, Harald and Greta Jeanssons Foundation, Novo Nordisk Foundation, O.E. and Edla Johanssons Scientific Foundation, the Swedish Cancer Society, the Swedish Diabetes Association, and the Swedish Research Council.

Received: September 12, 2007
Revised: January 11, 2008
Accepted: June 13, 2008
Published: July 1, 2008

REFERENCES

Abdel-Halim, S.M., Guenifi, A., Khan, A., Larsson, O., Berggren, P.O., Östenson, C.G., and Efendic, S. (1996). Impaired coupling of glucose signal to the exocytotic machinery in diabetic GK rats: a defect ameliorated by cAMP. Diabetes *45*, 934–940.

Ämmälä, C., Ashcroft, F.M., and Rorsman, P. (1993). Calcium-independent potentiation of insulin release by cyclic AMP in single beta-cells. Nature *363*, 356–358.

Berenjian, S., and Akusjärvi, G. (2006). Binary AdEasy vector systems designed for Tet-ON or Tet-OFF regulated control of transgene expression. Virus Res. *115*, 16–23.

Bergsten, P., Grapengiesser, E., Gylfe, E., Tengholm, A., and Hellman, B. (1994). Synchronous oscillations of cytoplasmic Ca^{2+} and insulin release in glucose-stimulated pancreatic islets. J. Biol. Chem. *269*, 8749–8753.

Charles, M.A., Fanska, R., Schmid, F.G., Forsham, P.H., and Grodsky, G.M. (1973). Adenosine 3′,5′-monophosphate in pancreatic islets: glucose-induced insulin release. Science *179*, 569–571.

Chow, R.H., Lund, P.E., Löser, S., Panten, U., and Gylfe, E. (1995). Coincidence of early glucose-induced depolarization with lowering of cytoplasmic Ca^{2+} in mouse pancreatic beta-cells. J. Physiol. *485*, 607–617.

Dachicourt, N., Serradas, P., Giroix, M.H., Gangnerau, M.N., and Portha, B. (1996). Decreased glucose-induced cAMP and insulin release in islets of diabetic rats: reversal by IBMX, glucagon, GIP. Am. J. Physiol. *271*, E725–E732.

Davis, B., and Lazarus, N.R. (1972). Insulin release from mouse islets. Effect of glucose and hormones on adenylate cyclase. Biochem. J. *129*, 373–379.

Delmeire, D., Flamez, D., Hinke, S.A., Cali, J.J., Pipeleers, D., and Schuit, F. (2003). Type VIII adenylyl cyclase in rat beta cells: coincidence signal detector/generator for glucose and GLP-1. Diabetologia *46*, 1383–1393.

Dunn, T.A., Wang, C.T., Colicos, M.A., Zaccolo, M., DiPilato, L.M., Zhang, J., Tsien, R.Y., and Feller, M.B. (2006). Imaging of cAMP levels and protein kinase A activity reveals that retinal waves drive oscillations in second-messenger cascades. J. Neurosci. *26*, 12807–12815.

Dyachok, O., and Gylfe, E. (2004). Ca^{2+}-induced Ca^{2+} release via inositol 1,4,5-trisphosphate receptors is amplified by protein kinase A and triggers exocytosis in pancreatic beta-cells. J. Biol. Chem. *279*, 45455–45461.

Dyachok, O., Isakov, Y., Sågetorp, J., and Tengholm, A. (2006). Oscillations of cyclic AMP in hormone-stimulated insulin-secreting beta-cells. Nature *439*, 349–352.

Edholm, D., Molin, M., Bajak, E., and Akusjärvi, G. (2001). Adenovirus vector designed for expression of toxic proteins. J. Virol. *75*, 9579–9584.

Eliasson, L., Ma, X., Renstrom, E., Barg, S., Berggren, P.O., Galvanovskis, J., Gromada, J., Jing, X., Lundquist, I., Salehi, A., et al. (2003). SUR1 regulates PKA-independent cAMP-induced granule priming in mouse pancreatic B-cells. J. Gen. Physiol. *121*, 181–197.

Gilon, P., Shepherd, R.M., and Henquin, J.C. (1993). Oscillations of secretion driven by oscillations of cytoplasmic Ca^{2+} as evidences in single pancreatic islets. J. Biol. Chem. *268*, 22265–22268.

Gorbunova, Y.V., and Spitzer, N.C. (2002). Dynamic interactions of cyclic AMP transients and spontaneous Ca^{2+} spikes. Nature *418*, 93–96.

Grapengiesser, E., Berts, A., Saha, S., Lund, P.E., Gylfe, E., and Hellman, B. (1993). Dual effects of Na/K pump inhibition on cytoplasmic Ca^{2+} oscillations in pancreatic beta-cells. Arch. Biochem. Biophys. *300*, 372–377.

Grill, V., and Cerasi, E. (1973). Activation by glucose of adenyl cyclase in pancreatic islets of the rat. FEBS Lett. *33*, 311–314.

Grynkiewicz, G., Poenie, M., and Tsien, R.Y. (1985). A new generation of Ca^{2+} indicators with greatly improved fluorescence properties. J. Biol. Chem. *260*, 3440–3450.

Haugh, J.M., Codazzi, F., Teruel, M., and Meyer, T. (2000). Spatial sensing in fibroblasts mediated by 3′ phosphoinositides. J. Cell Biol. *151*, 1269–1280.

He, T.C., Zhou, S., da Costa, L.T., Yu, J., Kinzler, K.W., and Vogelstein, B. (1998). A simplified system for generating recombinant adenoviruses. Proc. Natl. Acad. Sci. USA *95*, 2509–2514.

Hellman, B., Idahl, L.Å., Lernmark, Å., and Täljedal, I.B. (1974). The pancreatic beta-cell recognition of insulin secretagogues: does cyclic AMP mediate the effect of glucose? Proc. Natl. Acad. Sci. USA *71*, 3405–3409.

Hellman, B., Gylfe, E., Bergsten, P., Grapengiesser, E., Lund, P.E., Berts, A., Tengholm, A., Pipeleers, D.G., and Ling, Z. (1994). Glucose induces oscillatory Ca^{2+} signalling and insulin release in human pancreatic beta cells. Diabetologia *37* (*Suppl 2*), S11–S20.

Henquin, J.C. (2000). Triggering and amplifying pathways of regulation of insulin secretion by glucose. Diabetes *49*, 1751–1760.

Idevall-Hagren, O., and Tengholm, A. (2006). Glucose and insulin synergistically activate PI3-kinase to trigger oscillations of phosphatidylinositol-3,4,5-trisphosphate in beta-cells. J. Biol. Chem. *281*, 39121–39127.

Jung, S.K., Kauri, L.M., Qian, W.J., and Kennedy, R.T. (2000). Correlated oscillations in glucose consumption, oxygen consumption, and intracellular free Ca^{2+} in single islets of Langerhans. J. Biol. Chem. *275*, 6642–6650.

Landa, L.R., Jr., Harbeck, M., Kaihara, K., Chepurny, O., Kitiphongspattana, K., Graf, O., Nikolaev, V.O., Lohse, M.J., Holz, G.G., and Roe, M.W. (2005). Interplay of Ca^{2+} and cAMP signaling in the insulin-secreting MIN6 beta-cell line. J. Biol. Chem. *280*, 31294–31302.

Lang, D.A., Matthews, D.R., Burnett, M., and Turner, R.C. (1981). Brief, irregular oscillations of basal plasma insulin and glucose concentrations in diabetic man. Diabetes *30*, 435–439.

Lembert, N., and Idahl, L.Å. (1998). Alpha-ketoisocaproate is not a true substrate for ATP production by pancreatic beta-cell mitochondria. Diabetes *47*, 339–344.

Liu, Y.J., Tengholm, A., Grapengiesser, E., Hellman, B., and Gylfe, E. (1998). Origin of slow and fast oscillations of Ca^{2+} in mouse pancreatic islets. J. Physiol. *508*, 471–481.

Longo, E.A., Tornheim, K., Deeney, J.T., Varnum, B.A., Tillotson, D., Prentki, M., and Corkey, B.E. (1991). Oscillations in cytosolic free Ca^{2+}, oxygen consumption, and insulin secretion in glucose-stimulated rat pancreatic islets. J. Biol. Chem. *266*, 9314–9319.

Luciani, D.S., Misler, S., and Polonsky, K.S. (2006). Ca^{2+} controls slow NAD(P)H oscillations in glucose-stimulated mouse pancreatic islets. J. Physiol. *572*, 379–392.

Miyazaki, J., Araki, K., Yamato, E., Ikegami, H., Asano, T., Shibasaki, Y., Oka, Y., and Yamamura, K. (1990). Establishment of a pancreatic beta cell line that retains glucose-inducible insulin secretion: special reference to expression of glucose transporter isoforms. Endocrinology *127*, 126–132.

Molin, M., and Akusjärvi, G. (2000). Overexpression of essential splicing factor ASF/SF2 blocks the temporal shift in adenovirus pre-mRNA splicing and reduces virus progeny formation. J. Virol. *74*, 9002–9009.

Molin, M., Shoshan, M.C., Öhman-Forslund, K., Linder, S., and Akusjärvi, G. (1998). Two novel adenovirus vector systems permitting regulated protein expression in gene transfer experiments. J. Virol. *72*, 8358–8361.

Nilsson, T., Schultz, V., Berggren, P.O., Corkey, B.E., and Tornheim, K. (1996). Temporal patterns of changes in ATP/ADP ratio, glucose 6-phosphate and cytoplasmic free Ca2+ in glucose-stimulated pancreatic beta-cells. Biochem. J. *314*, 91–94.

Philipson, L. (1961). Adenovirus assay by the fluorescent cell-counting procedure. Virology *15*, 263–268.

Prentki, M., and Matschinsky, F.M. (1987). Ca^{2+}, cAMP, and phospholipid-derived messengers in coupling mechanisms of insulin secretion. Physiol. Rev. *67*, 1185–1248.

Pyne, N.J., and Furman, B.L. (2003). Cyclic nucleotide phosphodiesterases in pancreatic islets. Diabetologia *46*, 1179–1189.

Rabinovitch, A., Renold, A.E., and Cerasi, E. (1976). Decreased cyclic AMP and insulin responses to glucose in pancreatic islets of diabetic Chinese hamsters. Diabetologia *12*, 581–587.

Reddy, R., Smith, D., Wayman, G., Wu, Z., Villacres, E.C., and Storm, D.R. (1995). Voltage-sensitive adenylyl cyclase activity in cultured neurons. A calcium-independent phenomenon. J. Biol. Chem. *270*, 14340–14346.

Renström, E., Eliasson, L., and Rorsman, P. (1997). Protein kinase A-dependent and -independent stimulation of exocytosis by cAMP in mouse pancreatic B-cells. J. Physiol. *502*, 105–118.

Santana de Sa, S., Ferrer, R., Rojas, E., and Atwater, I. (1983). Effects of adrenaline and noradrenaline on glucose-induced electrical activity of mouse pancreatic beta cell. Q. J. Exp. Physiol. *68*, 247–258.

Schuit, F.C., and Pipeleers, D.G. (1985). Regulation of adenosine 3′,5′-monophosphate levels in the pancreatic B cell. Endocrinology *117*, 834–840.

Schuit, F.C., and Pipeleers, D.G. (1986). Differences in adrenergic recognition by pancreatic A and B cells. Science *232*, 875–877.

Schulze, D.U., Dufer, M., Wieringa, B., Krippeit-Drews, P., and Drews, G. (2007). An adenylate kinase is involved in K_{ATP} channel regulation of mouse pancreatic beta cells. Diabetologia *50*, 2126–2134.

Seino, S., and Shibasaki, T. (2005). PKA-dependent and PKA-independent pathways for cAMP-regulated exocytosis. Physiol. Rev. *85*, 1303–1342.

Sharp, G.W. (1979). The adenylate cyclase-cyclic AMP system in islets of Langerhans and its role in the control of insulin release. Diabetologia *16*, 287–296.

Takahashi, N., Kadowaki, T., Yazaki, Y., Ellis-Davies, G.C., Miyashita, Y., and Kasai, H. (1999). Post-priming actions of ATP on Ca^{2+}-dependent exocytosis in pancreatic beta cells. Proc. Natl. Acad. Sci. USA *96*, 760–765.

Tarasov, A.I., Girard, C.A., and Ashcroft, F.M. (2006). ATP sensitivity of the ATP-sensitive K^+ channel in intact and permeabilized pancreatic beta-cells. Diabetes *55*, 2446–2454.

Tengholm, A., Hellman, B., and Gylfe, E. (1999). Glucose regulation of free Ca^{2+} in the endoplasmic reticulum of mouse pancreatic beta cells. J. Biol. Chem. *274*, 36883–36890.

Tsuboi, T., and Rutter, G.A. (2003). Multiple forms of "kiss-and-run" exocytosis revealed by evanescent wave microscopy. Curr. Biol. *13*, 563–567.

Valdeolmillos, M., Santos, R.M., Contreras, D., Soria, B., and Rosario, L.M. (1989). Glucose-induced oscillations of intracellular Ca^{2+} concentration resembling bursting electrical activity in single mouse islets of Langerhans. FEBS Lett. *259*, 19–23.

Valverde, I., Vandermeers, A., Anjaneyulu, R., and Malaisse, W.J. (1979). Calmodulin activation of adenylate cyclase in pancreatic islets. Science *206*, 225–227.

Westerlund, J., Gylfe, E., and Bergsten, P. (1997). Pulsatile insulin release from pancreatic islets with nonoscillatory elevation of cytoplasmic Ca^{2+}. J. Clin. Invest. *100*, 2547–2551.

Willoughby, D., and Cooper, D.M. (2006). Ca^{2+} stimulation of adenylyl cyclase generates dynamic oscillations in cyclic AMP. J. Cell Sci. *119*, 828–836.

Wollheim, C.B., and Sharp, G.W. (1981). Regulation of insulin release by calcium. Physiol. Rev. *61*, 914–973.